Fatigue assessment of welded joints considering residual stresses due to welding process and post weld treatment

Peter Schaumann[a], Christian Keindorf[a], Mareike Mickley[b]

[a] Institute for Steel Construction, Leibniz University Hannover, Germany
[b] University of British Columbia, BC, Vancouver, Canada V6T 1Z4

Abstract For welded joints subjected to dynamic loads fatigue resistance of the base material and the weld is very important to design steel constructions in fatigue limit state. In most cases residual stresses due to the welding process reduce the fatigue resistance. However, the fatigue strength can be enhanced by methods of post weld treatment. One of these is the Ultrasonic-Impact-Treatment (UIT), which introduces beneficial compressive stresses at the weld toe zones and reduces stress concentrations by improving the weld toe. Numerical simulations were carried out for seam butt welds using an arc welding process followed by a process of needle peening. The objective of numerical investigations was to analyse the influence of residual stresses on the fatigue life for welded steel plates with and without post weld treatment. The total fatigue life of such welded joints was assessed by adding crack initiation life calculated with notch strain approach and crack propagation life calculated with crack propagation approach.

1 INTRODUCTION

The fatigue resistance of welded joints can be enhanced by post weld treatment. One method for this is Ultrasonic Impact Treatment (UIT). It is a proprietary technology developed originally in the Soviet Union for use on naval ships to reduce welding stresses (STATNIKOV et al., 1977). The equipment comprises a handheld tool and an electronic control box (Fig. 1). The tool is easy to handle during application. It operates at the head movement with a mechanic frequency of 200 Hz overlain by an ultrasonic frequency of 27000 Hz. The noise is negligible compared to other peening devices. Several kinds of heads and pins are available and can be chosen on the basis of the surface condition of the weld details to be treated. The method involves post-weld deformation treatment of weld toe by impacts from single or multiple indenting needles excited at ultrasonic frequency, generating mechanic impulses on the work surface (STATNIKOV et al., 1997). The objective of the treatment is to introduce beneficial compressive residual stresses at the weld toe zones and to reduce stress concentration by improving the weld toe profile. Furthermore, the area being treated is highly plastically deformed which has the effect of work hardening. Compared to other impact treatment methods such as air hammer peening, shot peening or needle peening, UIT is claimed to be more efficient involving a complex effect of strain hardening, reduction in weld strain, relaxation in residual stresses reduction in stress concentration and thereby achieving a deeper cold worked metal layer (STATNIKOV et al., 1997).

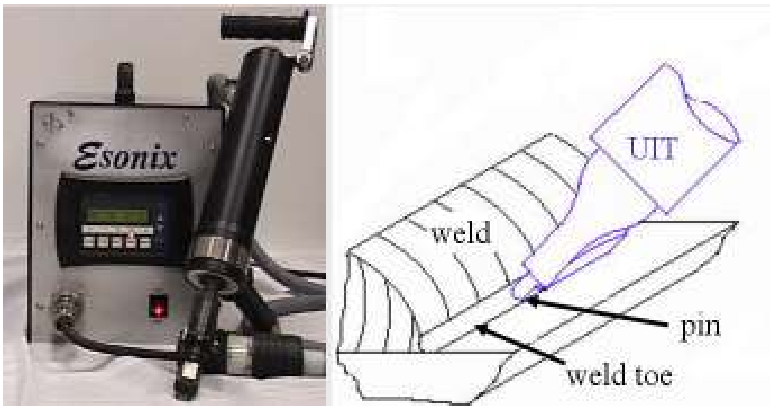

Figure 1. Ultrasonic Impact Treatment (UIT) [Applied Ultrasonics Europe].

This paper deals with the numerical simulation of both the welding process as well as the post weld treatment. The purpose is to quantify the positive effects on the distribution of residual stresses adjacent to the weld toe and consequently on the fatigue resistance of the weld assessed by local concepts.

2 NUMERICAL SIMULATION OF WELDING AND UIT-PROCESS

For detailed numerical analyses of UIT-effects the process of welding was coupled with the post weld treatment process for two steel plates with a single butt weld. The symmetric half model, implemented in ANSYS®, consists of three zones the weld, the heat affected zone and the base material of the steel plate (Fig. 2). The dimensions of the steel plate fabricated from S355 J2G3 are 100 x 100 x 6 mm. Material properties are implemented depending on temperature. The notch at the weld toe has a variable radius to consider the actual weld geometry for as welded and treated conditions. The smallest dimension of an element at the notch has been chosen to 0.2 mm in direction of thickness. The model was driven by displacement boundary conditions.

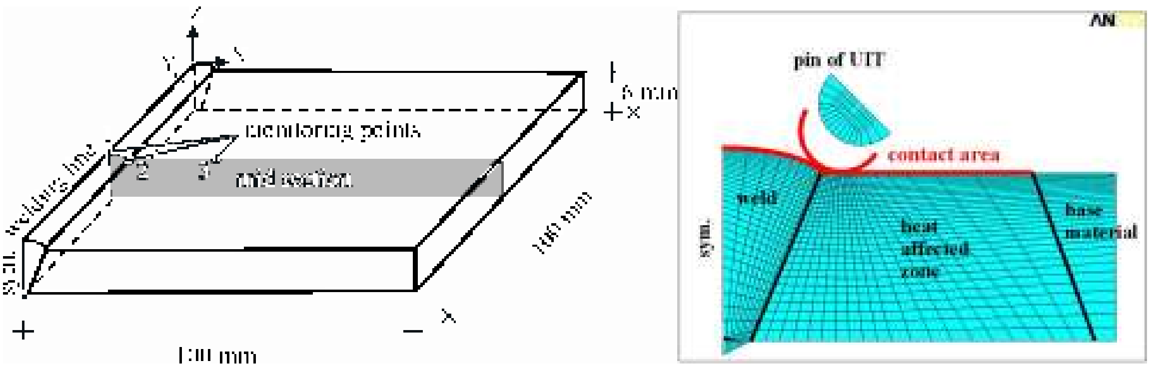

Figure 2. Geometry and FE-model of a steel-plate with a single butt weld.

With this FE-model two main effects have been investigated. Firstly, the transient field of residual stresses due to welding and post weld treatment has been simulated. Secondly the change in geometry of weld profile has been calculated. Both effects have a significant influence on the fatigue life of the welded joints. To simulate the post weld treatment the penetration of the 3 mm diameter pin of the UIT handheld tool into the weld toe has been calculated as illustrated in Figure 2.

2.1 Thermal analysis of welding process

The simulation of the welding process consists of two of analyses. At first, the transient field of temperature has to be calculated during arc welding process. After the transient thermal analysis the structural analysis has to be carried out to determine the residual stresses. For the transient thermal analysis a half symmetric steel plate having a length of 100 mm (welding direction), width of 100 mm and thickness of 6 mm was modeled with 3D-thermal elements (Solid70). These elements have eight nodes with a single degree of freedom, temperature, at each node. The butt weld was generated as single pass welding process with a welding speed of v_{weld} = 5 mm/s. The electric input was U = 23.5 V and I = 165 A, and the arc efficiency was assumed to be η = 90 %. Parametric meshing was used in order to easily track the results along a certain predefined path in any direction. For thermal symmetry the heat flux passing across the surface of symmetry shown in Figure 12 was assumed to be zero, and, for structural symmetry, the translation in the x-direction of the same surface was also zero. It is important to note that the automatically estimated time increment in the analysis dropped to a very small value due to the vast difference in the temperatures. This effect can be dramatic for small element-size of the weld pool at the fusion surface the parting surface. But the meshing in the weld pool must be fine enough to account for the high temperature gradient calculation. The transient temperature profile during the welding process was analyzed using Goldak's formulation of the double-ellipsoidal heat source (GOLDAK, 1984). The total heat input Q has been evaluated according to electric arc welding with $Q = \eta \cdot U \cdot I$. The heat flux q was applied in the model to calculate the thermal load at a certain time and location within the volume of elements according to Eq. (1)

$$q_{vol}(x,y,z) = q_{\max} \cdot e^{-3\left(\frac{x^2}{a^2}+\frac{y^2}{b^2}+\frac{z^2}{c^2}\right)} \tag{1}$$

where q_{vol} = heat flux in a volume, q_{max} = maximum heat flux in the center; x, y, z = distance from the center point of heat source and a, b, c = distance with 5 % of q_{max} for limiting the heat source. The form of the heat source for electrical arc welding using Goldak's formulation is shown in Figure 3a for example in a single block.

In the beginning the heat source was located at one edge of the plate in y_0 = 0 mm at time t_0 = 0 s taken for the center point of the heat to reach the first node. The motion of the heat load zone along the welding line was considered by $y_{source} = y_0 + t \cdot v_{weld}$. Thus, with increasing time, y_{source} increase along the welding line as shown in Figure 3a.

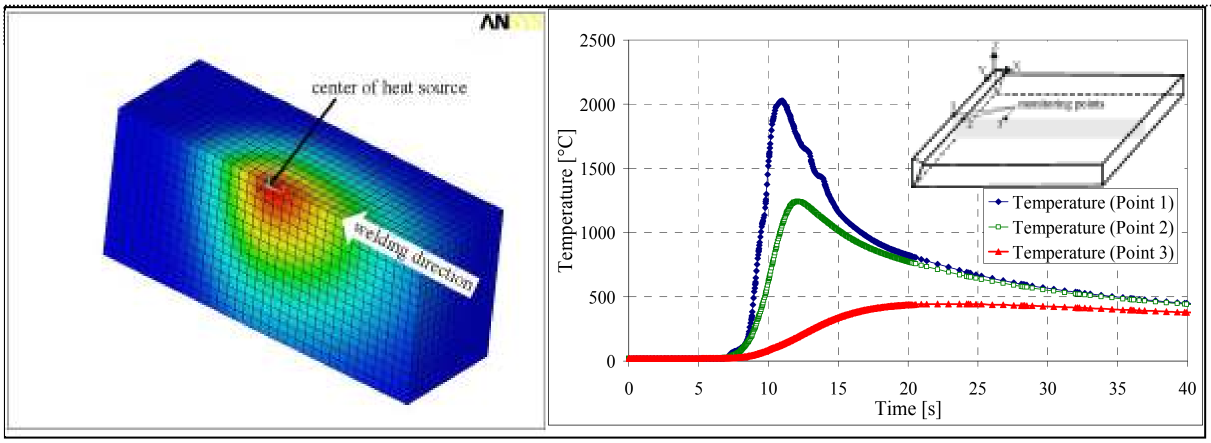

Figure 3. (a) Moving heat source for electrical arc welding and (b) Temperature history

The thermal boundary conditions include the radiation and convection to the environment from all sides of the welded plate except the symmetry surface. The results of the transient thermal analysis are presented in Figure 3b for three monitoring points indicated in Figure 1 along the mid transverse line on the top surface. The monitoring point 1 is located at the welding line, point 2 at the weld toe and point 3 has a distance of 10 mm perpendicular to the weld toe. The maximum temperature of point 1 was $T_{1,max}$ = 2025 °C at t = 11 s shortly after the center of the heat source reached the mid section. At the same time the weld toe had a temperature of T_2 = 1070 °C. It could be seen that the temperature curves rose highly for the points when the heat source was passing both points. The point 3 is located in the heat affected zone with a maximum temperature of $T_{3,max}$ = 445 °C. The cooling process was terminated at nearly t = 2000 s.

2.2 Structural analysis of welding process

After thermal analysis the element type in ANSYS® has been changed from Solid70 to Solid45. For structural boundary conditions the surface at x = 100 mm shown in Figure 1 was constrained in x, y and z-direction. In addition the translation in x-direction at the surface of symmetry (x = 0) was also zero. The metal deposition of the filler material was considered using the element birth technique. This technique is based on deactivating and reactivating the elements of the weld pool as the welding progresses. The meshing of the base plate and the butt weld had a clear parting surface between them. The nodal temperatures over time determined in thermal analysis were the load for the subsequent structural analysis of the welding process. The simulation was carried out up to t = 2000 s to estimate the residual stresses during the cooling period. The final residual stress distribution transverse to the welding line (sx) is shown in Figure 4a. The maximum transverse stress is located at the weld toe with values in tension near the yield stress. Because of this high residual stress state the weld toe is often the area where the fatigue crack is initiated.

2.3 Contact analysis of post weld treatment

The post weld treatment by UIT was considered using a contact algorithm with element types CONTA173 and TARGE 170. For the simulation only the top of the UIT-pin shown in Figure 2 was modelled. The pin was positioned in the mid section with an initial gap to the base plate. After restarting the transient structural analysis the pin moved in an angle of 60° to the weld toe and deformed this surface. The residual stress state in x-direction after post weld treatment is shown in Figure 4 (right).

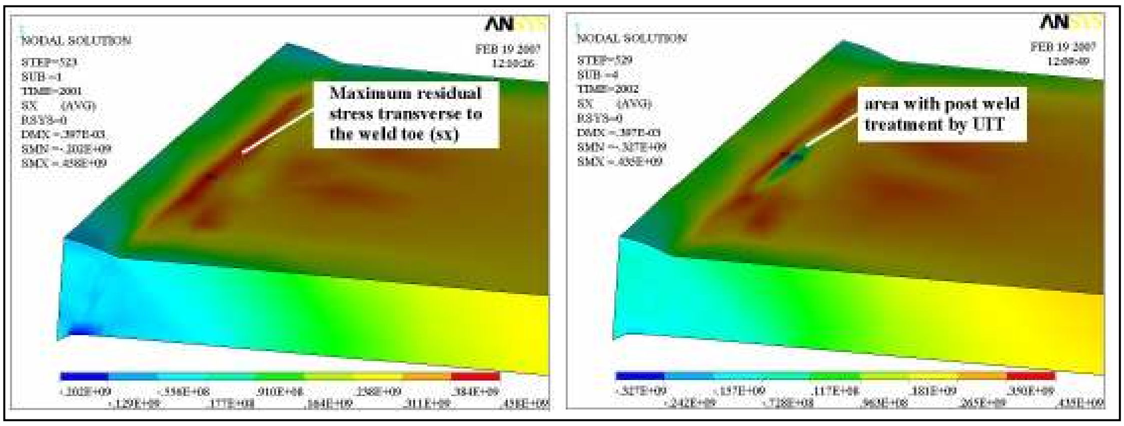

Figure 4. Residual stresses transverse to the weld toe before (left) and after (right) post weld treatment.

The transverse stress in the treated area changed from tensile residual stresses (σ_{R,T,as_welded} = +458 N/mm²) to compressive residual stresses near the yield stress ($\sigma_{R,T,uit}$ = -327 N/mm²). Due to introduced compressive stresses which are one effect of UIT the fatigue strength increased significantly compared to as welded. Furthermore, the weld geometry was rounded by the pin and the toe notch radius increased. The residual stress distribution transverse to the weld toe was compared in Figure 5 (left) for the as welded and treated conditions in mid section. The transverse stress distribution for the as welded condition rises up from the welding line (monitoring point 1) to the maximum value at the toe (monitoring point 2) and decreased slowly to a stress level of 300 N/mm² in the base plate (monitoring point 3). In contrast to the as welded situation the stress distribution after post weld treatment had a negative peak located at the weld toe. The compressive stress reacheed a minimum value of -280 N/mm². In the near of the peak the residual stress were also reduced. But with more distance to the welding line the curve reached the stress level like in the as welded condition. The local treatment at the toe in mid section reduced also the residual stresses along the weld toe line. This effect is noticed for the longitudinal stresses presented in Figure 5 (right). The longitudinal stress distribution in as welded condition increased from the edges of the plate to a stress plateau nearly 220 N/mm² in the mid section. This stress behaviour is typical for arc welding of two coplanar plates with a butt weld processed as single pass. After cooling period was finished the weld toe was treated by UIT. There the pin was positioned in the toe area from y = 40 – 60 mm. The longitudinal residual stresses are reduced significantly with a minimum value of -220 N/mm² in the treated area. The maximum penetration reached a value of 0.1 mm.

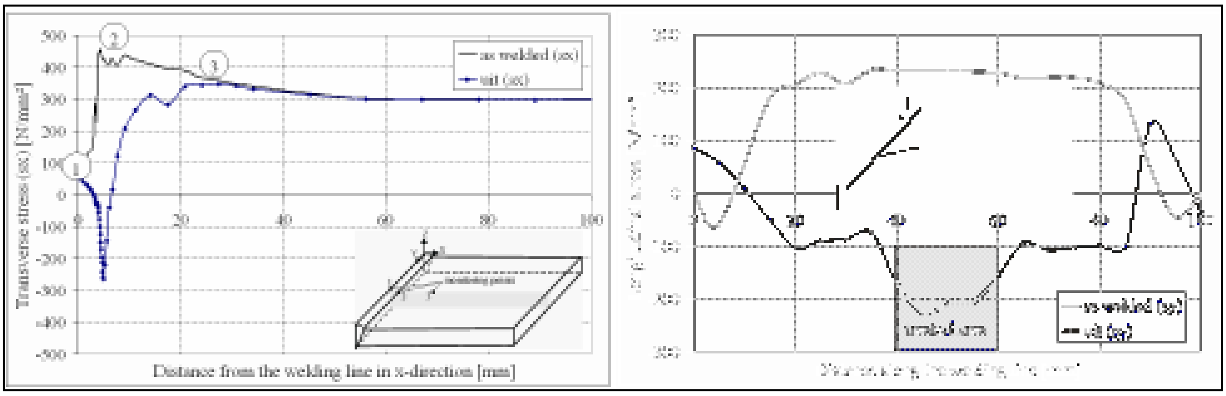

Figure 5. Comparison of residual stresses before (left) and after (right) post weld treatment.

Finally it can be noticed that the post weld treatment by UIT has a great influence on the local stress state at the weld toe which is often the position for crack initiation. Due to introduction of compressive residual stress and plastic deformations at the top surface micro cracks can be closed. The numerical results are suitable to assess the fatigue strength under consideration of the modified residual stress state at the weld toe.

3 FATIGUE ASSESSMENT UNTIL CRACK INITIATION

3.1 Theory of notch strain approach

The notch strain approach is used for assessing the fatigue strength of the welded joint up to technical crack initiation. The idea behind this approach is that the mechanical behaviour of the material at the notch root in respect of local damage is similar to the behaviour of a miniaturized, axially loaded, unnotched specimen in respect of global damage. The comparison specimen is assumed to be positioned at the notch root. It should have the same microstructure, the same surface condition inclusive of residual stresses and, if possible, the same volume as the highly stressed material at the notch root (RADAJ, SONSINO, FRICKE, 2006).

3.2 Basic formulae according to version of Seeger

The following equations are basic formulae for the strain notch approach according to the version of SEEGER. At first the cyclic stress-strain curves according to RAMBERG and OSGOOD have to be described by:

$$\varepsilon_a = \varepsilon_{a,el} + \varepsilon_{a,pl} = \frac{\sigma_a}{E} + \left(\frac{\sigma_a}{K'}\right)^{1/n'} \tag{2}$$

where ε_a = total strain amplitude; $\varepsilon_{a,el}$ = elastic strain amplitude; $\varepsilon_{a,pl}$ = plastic strain amplitude; σ_a = stress amplitude; E = elastic modulus; K´ = cyclic strain-hardening coefficient and n´ = cyclic strain-hardening exponent.

The strain S-N curve according to MANSON and COFFIN including the mean stress effect to MORROW describing technical crack initiation is given by

$$\varepsilon_a = \frac{\sigma'_f - \sigma_m}{E}(2N)^b + \varepsilon'_f (2N)^c \qquad for \quad (N \leq N_E) \tag{3}$$

where σ_f' = fatigue strength coefficient; ε_f' = fatigue ductility coefficient; b = fatigue strength exponent; c = fatigue ductility exponent; σ_m = mean stress; N = number of cycles up to crack initiation and N_E = number of cycles at the technical endurance limit.

The cyclic material parameters in Eqs. (2) and (3) are presented by BÄUMEL & SEEGER 1990 for non welded base metals according to the uniform material law, shown in Table I:

Table I. Cyclic material parameters according to BÄUMEL & SEEGER.

Material parameters	basic formulae for steel, unalloyed and low-alloy	S 355 J2G3
σ_u	R_m	510
σ_f'	$1.50 \cdot \sigma_u$	765
b	-0.087	-0.087
ε_f'	0.59 ψ	0.59
c	-0.58	-0.58
σ_E^b	$0.45 \cdot \sigma_u$	229.5
ε_E^b	$0.45 \cdot \sigma_u/E + 1.95 \cdot 10^{-4} \cdot \psi$	$1.287 \cdot 10^{-3}$
N_E	$5 \cdot 10^5$	$5 \cdot 10^5$
K'	$1.65 \cdot \sigma_u$	841.5
n'	0.15	0.15
ψ	ψ =1.0 for $\sigma_u/E \leq 3 \cdot 10^{-3}$	1.0
	ψ =(1.375-1.25 σ_u/E) ≤ 0 for $\sigma_u/E > 3 \cdot 10^{-3}$	

The curve branches of the stress-strain hysteresis loop, rising or dropping from the cusp point, are described according to MASING by:

$$\varepsilon = \varepsilon_a + \frac{\sigma - \sigma_a}{E} + 2\left(\frac{\sigma - \sigma_a}{2K'}\right)^{1/n'} \tag{4}$$

where σ and ε = stress and strain on the hysteresis curve branch; σ_a = stress amplitude; E = elastic modulus; K' = cyclic strain-hardening coefficient and n' = cyclic strain-hardening exponent. The stresses and strains at the notch root in the elastic-plastic state, according to NEUBER as macro-structural support formulae is given by:

$$\sigma_k \varepsilon_k = \left(\frac{\sigma_n \cdot K_t}{E}\right)^2 \tag{5}$$

where σ_k and ε_k = maximum notch stress and strain in the elastic plastic state; σ_n = nominal stress; E = elastic modulus; K_t = elastic stress concentration factor.

The elastic stress concentration factor K_t for the weld toe geometry was determined numerically for as welded and also for treated condition. The notch radius for as welded is considered according to RADAJ with r = 1 mm and for the treated toe with r = 1.5 mm. In test series with Y-joints a notch radius of r_{uit} = 1.8 mm was measured, but for idealized the radius for UIT is assumed theoretically to the radius of the pin with r_{pin} = 1.5 mm. The detailed notch geometry is presented in Figure 6 with the corresponding smooth comparison specimen at the notch root.

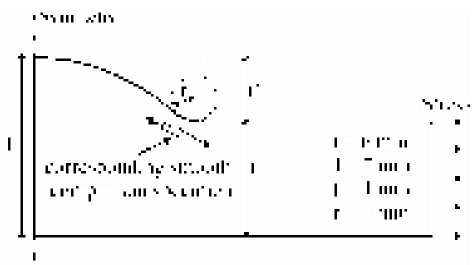

Figure 6. Geometry of the butt weld.

In addition to the numerical solution the elastic stress concentration factor K_t can be calculated with the following formulae given in FKM Guideline 2002:

$$K_t = 1 + \frac{1}{\sqrt{0.5\frac{r}{t} + 5\frac{r}{t}\left(1 + 2\frac{r}{t}\right)^2}} \quad (6)$$

where K_t = elastic stress concentration factor; r = notch radius and t = thickness of plate.

The comparison of the numerical and analytical results is shown in Table II. The results agree well for both conditions.

Table II. Comparison of elastic stress concentration factor.

weld toe	notch radius r	elastic stress concentration factor K_t	
	[mm]	analytical	numerical
as welded	1.0	1.72	1.66
UIT	1.5	1.53	1.57

Local residual stresses have to be taken into account when determining the stress-strain hysteresis loops by the elastic-plastic analysis. This analysis can be based on a modification of NEUBER'S macrostructural support formula:

$$\sigma_k(\varepsilon_k - \varepsilon_r) = \frac{1}{E}(\sigma_n \cdot K_t)^2 \quad (7)$$

where σ_k and ε_k = maximum notch stress and strain in the elastic plastic state; σ_n = nominal stress; E = elastic modulus; K_t = elastic stress concentration factor and $\varepsilon_r = \sigma_r / E$ initial local residual strain.

The damage parameter P-N curves comprise the effect of mean stress σ_m on the S-N curve with respect to technical crack initiation. Thus, the damage parameter P allows the conversion of a stress-strain hysteresis loop with non-zero mean stress into a damage-equivalent loop with zero mean stress. The damage parameter P_{SWT} most often used has been defined for uniaxial loading by SMITH, WATSON and TOPPER. For each load cycle j the corresponding number cycles N_j must be assessed. After that, the damage contributions of the hysteresis loops are determined linear by PALMGREN-MINER rule for each load cycle j. In the end all partial damages add themselves until the total damage is equal to 1.0.

3.3 Estimation of fatigue life until crack initiation

The crack initiation life was calculated based on the notch strain approach using the version of SEEGER. The S-N curve was determined with the damage parameter P_{SWT} assuming the material properties of the base material. Elastic-plastic behaviour, residual stresses and the different elastic stress concentration factors for both conditions were taken into account. The predicted S-N curves for crack initiation of butt weld are presented in Figure 7.

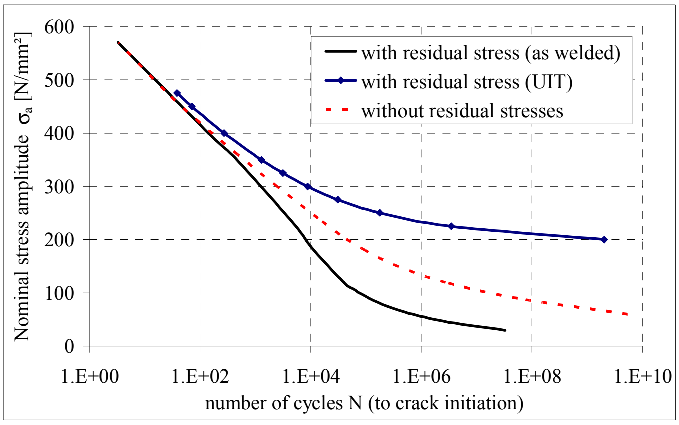

Figure 7. Predicted S-N curves for crack initiation.

In Figure 7 the numbers of cycles N is plotted against the nominal stress amplitude σ_a for alternating loading (R = -1). The curve for as welded condition has the lowest fatigue strength because of the tensile residual stresses. In contrast to as welded condition the butt weld with the treated toe has higher fatigue strength. The post weld treatment introducing compressive stresses in the notch root is highly effective in this case. The analysis indicates that the influence of residual stresses at the weld toe is significant for the crack initiation life. The results for both conditions are compared with the S-N curve without considering residual stresses which S-N curve is obviously between these both cases. Finally, the results are shown graphically as plots using the tool which is implemented in ANSYS®. On that it is extended on the consideration of residual stresses according to SEEGER'S attempt of residual stresses in thin surface layers and according to LAWRENCE characterization of residual stresses as mean stress. For the application of this tool, it has to be mentioned critically that the iterations for the elastic-plastic stress-strain behaviour at notch and finally the one for getting life cycle is very time-consuming in the calculation. To save computing time the accuracy for the iteration of stress-strain path at notch is set to $\Delta\sigma = 0.1$ MPa and for the iteration of life cycle to $\Delta N = 500$. This means in every step of iteration the stress or number of cycle is raised by this delta value. The amplitude is set to $\sigma_a = 0.5 \cdot \sigma_y = 180.0$ MPa with a stress range $R = -1$ and $\sigma_m = 0.0$ MPa. Besides, for getting adequate results there is a need for fine meshing especially at crack critical sites at the weld toe. That is why these plots can only be used for qualitative illustrations and considerations at which locations the number of life cycles are critical and cracks may be initiated.

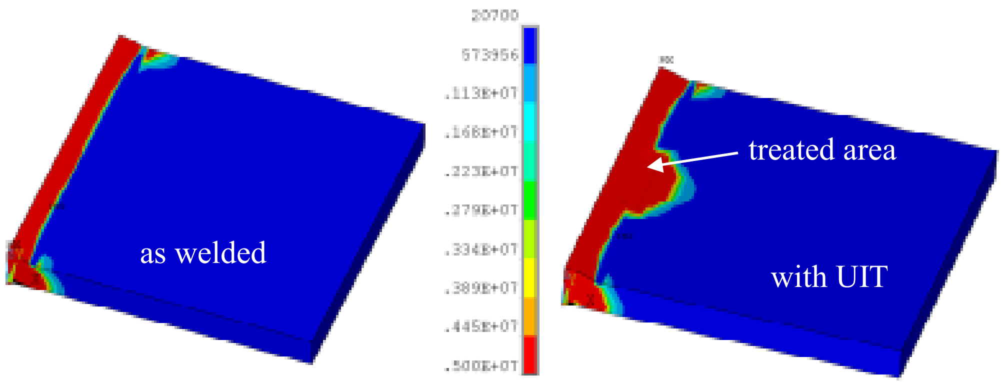

Figure 8. Number of cycles until crack initiation for as welded (left) and treated condition (right).

As expected for the butt-welded plate the critical location for crack initiation is at the weld toe (Fig. 8 left). Figure 8 right shows the weld after treatment with UIT. To evaluate the effect of UIT the region of static pressing of bolt has to be regarded. It has to be mentioned that only the midsection of the weld toe line was treated. In this process the pin of UIT was positioned in the toe area from y = 40 – 60 mm. In this case the location of crack initiation moves away from the weld toe. Despite of treatment with UIT, in most cases failure of component occurs still at weld toe or in some cases also in the base material.

4 FATIGUE ASSESSMENT FOR CRACK PROPAGATION

The fatigue life of structural members with an existing crack or gap can be calculated according to the crack propagation approach. Basically, two starting points for the application of the crack propagation approach may be distinguished. On the one hand the crack defect already exist and can be measured by non-destructive tests, or on the other hand following the notch strain approach and the initiation of a so called 'technical' crack. This one has been pursued in the following under consideration of peculiarities of seam-welded joints. Basis is again the butt-welded plate of the chapter before. Finally, the total fatigue life for this connection under consideration of residual stresses due to welding and post weld treatment can be determined. For welded joints the primary concern of the crack propagation approach is directed towards surface cracks at areas of notch stress concentration such as weld toes. In most cases these are semi-elliptical surface cracks.

4.1 Stress intensity factor for welded joints

The most important factor for describing the fatigue action at the crack tip is the stress intensity factor range ΔK. A suggestion for butt-welded joints according to HOBBACHER is chosen for this kind of application. HOBBACHER et al. split the universal correction function $Y_u(a)$ into a function $Y(a)$, which refers to a solution of a standard crack configuration, and a second function $M_k(a)$, which describes the correction due to the local stress concentration of the weld.

$$K = \sigma \cdot \sqrt{\pi \cdot a} \cdot Y_u(a) = \sigma \cdot \sqrt{\pi \cdot a} \cdot Y(a) \cdot M_k(a) \quad (8)$$

4.2 Residual stresses

Residual stresses may influence crack propagation behaviour essentially. Tensile residual stresses normal to crack surfaces cause that the crack remains open. In contrast, compression residual stresses have a positive effect on crack propagation life. These stresses induce early crack closure. RADAJ proposed for the consideration of residual stresses due to welding process through an effective stress range R_{eff} which can be calculated with following equation

$$R_{eff} = \frac{f_y - \Delta\sigma}{f_y} \tag{9}$$

Therefore, due to welding process residual stresses near the yield limit σ_y are assumed. In most cases the stress range $\Delta\sigma$ is smaller than residual stresses in regions of yield limit. In turn means, that the stress ratio R_{eff} remains positive and crack closure effects due to stress range in compression regions does not have to be considered. Residual stress can also be considered directly by the stress intensity factor K_I.

$$K_{res} = Y(a) \cdot \sqrt{\frac{a}{\pi}} \cdot \int_0^a \frac{\sigma_{res}}{\sqrt{a^2 - x^2}} dx \tag{10}$$

Therefore, the function of residual stresses σ_{res} has to be known. The modified FORMAN equation which can be used for flaw growth parameters C and m is chosen according to PARIS. Often R = 0.5 is assumed to consider residual stresses due to the welding process. In combination with post weld treatment compression stresses are of special interest. Compressive stresses can reduce the weld induced stress, which reduces the stress ratio R as well. With R < 0 the threshold is significantly increased, so compressive stresses induced by post weld treatment can prevent weld toe fatigue crack initiation, if the stress range is low, or delay it for high stress ranges. This beneficial effect has been observed in fatigue tests. But if compressive stress layer is only shallow and a crack initiates from the treated weld toe the favourable compressive stresses are released. According to CHENG then fatigue growth is nearly as the original non-treated weld toe. In this way it can be suggested that post weld treatment has greater effect on crack initiation and early propagation (stage I) rather than stage II of fatigue crack propagation.

4.3 Crack propagation

In dependence of the input data the crack growth equation different possibilities can be chosen. The simplest and at the furthest common equation is the one according to PARIS. It can get necessary of the consideration of different stress ratio R, the threshold value of stress intensity K_{th}, or fracture toughness K_c to use different modifications of the Paris equation and also according to FORMAN or NEWMAN. This has to be decided in the individual case and for more reliable results in connection with experimental tests in a lab or measurements on-site.

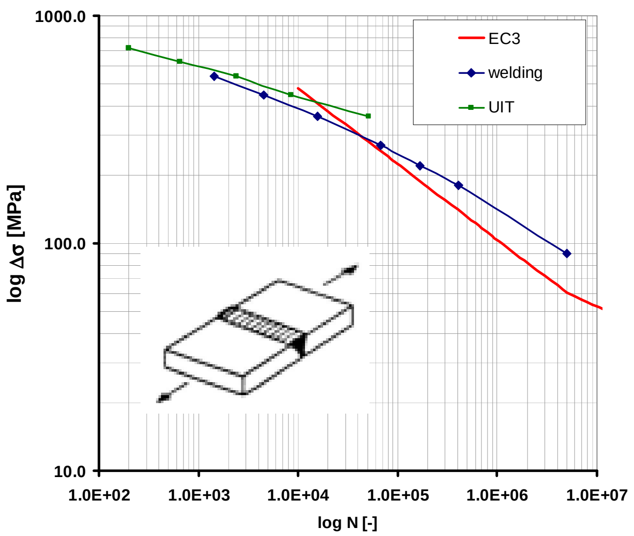

Figure 9. Predicted SN-curves for total fatigue life.

For the calculations in this section crack growth equations according to PARIS and FORMAN have been chosen. The used parameters are $C = 5.0 \cdot 10^{-13}$ $Nmm^{-3/2}$ and $m = 3$ for the flaw growth parameters and $K_c = 4000$ $Nmm^{-3/2}$ for fracture toughness. According to RADAJ, experimental tests for welded joints show for crack initiation a depth $a_i = 0.1$. To consider different ratios a/c in crack propagation the stress intensity factor according to NEWMAN has to be taken into account. Figure 9 shows the positive influence of post weld treatment on fatigue life, where the curves in as-weld and treated condition are compared. The slope of curve for UIT is less steep which means more cycles for the same stress level are possible.

5 CONLUSIONS

Under the point of view of fatigue resistance the welded joints represent the weak point of every very dynamically loaded steel construction. Induced residual stresses or changes in the crystalline structure due to heating are only two of many notch effects. In the underlying research project the Ultrasonic Impact Treatment (UIT) has been applied as a method of post weld treatment to improve fatigue resistance. Numerical simulations have been carried out for a butt weld seam using an arc welding process with a following process of needle peening, like UIT. The objective of the numerical investigations was analysing the influence of residual stresses on the fatigue life for welded joints with and without post weld treatment. The fatigue investigations until technical crack expelled that the crack is initiated at the weld toe in as-welded condition. After UIT-treating of the weld toe in the midsection the predicted location of crack initiation moved from the weld toe towards the heat affected zone. For the identified location of potential crack initiation the stage of crack propagation could be considered. For calculating the crack propagation a stress intensity factor has been chosen considering the residual stress effects for both conditions. Finally, the total fatigue life has been assessed as the sum of crack initiation life calculated with the notch strain approach and crack propagation life calculated with the crack propagation approach. The increase of the fatigue resistance due to UIT post weld treatment known from experimental investigations could be comprehended also by numerical simulation. The appropriate S-N-curve obtains both a higher detail category as well as a flatter slope compared to the as-welded condition.

6 REFERENCES

6.1 Book

1. D. Radaj, C. M. Sonsino, W. Fricke, Fatigue assessment of welded joints by local approaches, Second edition, Woodhead Publishing Limited and CRC Press LLC, 2006
2. A. Bäumel, T. Seeger, Materials Data for Cyclic Loading, Suppl. 1, Amsterdam, Elsevier Science, 1990

6.2 Conference Proceedings

3. P. Schaumann, C. Keindorf, Enhancing fatigue strength by ultrasonic impact treatment for welded joints of offshore structures, Third International Conference on Steel and Composite Structures (ICSCS07), 921-926, Manchester, UK, 2007.

6.3 Journal Article

4. X. Cheng, et al., Residual stress modification by post-weld treatment and its beneficial effect on fatigue strength of welded structures, International Journal of Fatigue 25, 1259-1269, Elsevier, 2003.
5. I. F. Z. Fanous, et al., 3-D Finite element modelling of the welding process using element birth and element movement techniques, ASME, Pressure Vessels and Piping Division, Vol. 125, USA, 2003.
6. E. S. Statnikov, et al., Applications of operational ultrasonic impact treatment (UIT) technologies in production of welded joints, IIW, Doc. XIII-1668-97, IIW, Paris, France, 1997.
7. A. Hobbacher, Stress intensity factors of welded joints, Welding Laboratory, FH Wilhelmshaven, Engineering Fracture Mechanics, Vol.46, No.2, 173-182, Pergamon Press Ldt., 1993.
8. J. Goldak, et. al., A new finite element model for welding heat sources, Metallurgical Transactions B, 15B, 299-305, 1984.
9. J. C. Newman, I. S. Raju, An empirical stress-intensity factor equation for the surface crack, NASA Langley Research Center, Hampton, USA, Engineering Fracture Mechanics, Vol.15, No.1-2, 185-192, Pergamon Press Ltd., 1981.
10. E. S. Statnikov, et al., Ultrasonic impact tool for strengthening welds and reducing residual stresses, New Physical Methods of Intensification of Technological Processes, 1977.

6.4 Thesis

11. M. Mickley, Fatigue resistance of welded joints considering residual stresses due to welding and post weld treatment, Diploma thesis, Institute for Steel Construction, Leibniz University Hannover, 2007.
12. S. Zacke, Numerische Simulation und Bewertung des transienten Eigenspannungsfeldes infolge eines Schweißprozesses mit anschließender UIT-Behandlung, Diploma thesis, Institute for Steel Construction, Leibniz University Hannover, 2007.

6.5 Standards, Codes and Guidelines

13. A. Hobbacher, Recommendations for fatigue design of welded joints and components, International Institute of Welding, IIW document XIII-1965-03 (draft for development), 2003.
14. FKM-Giudeline: Rechnerischer Festigkeitsnachweis für Maschinenbauteile aus Stahl, Eisenguss- und Aluminiumwerkstoffen; 4. Auflage, VDMA Verlag GmbH, Frankfurt, Germany, 2002.
15. Applied Ultrasonics, Esonix Ultrasonic Impact Treatment: Technical Procedure Document, Applied Ultrasonics, Birmingham, AL, USA, 2002.